Clinical Cancer Research

A Zebrafish Model Discovers a Novel Mechanism of Stromal Fibroblast-Mediated Cancer Metastasis

Caifeng Liu[1,2], Yunjian Zhang[1,3], Sharon Lim[1], Kayoko Hosaka[1], Yunlong Yang[1,4], Tatiana Pavlova[1], Twana Alkasalias[1], Johan Hartman[5], Lasse Jensen[1,6], Xiaoming Xing[7], Xinsheng Wang[7], Yongtian Lu[4], Guohui Nie[4], and Yihai Cao[1,4,7]

Abstract

Purpose: Cancer metastasis can occur at the early stage of tumor development when a primary tumor is at the microscopic size. In particular, the interaction of malignant cells with other cell types including cancer-associated fibroblasts (CAF) in promoting metastasis at the early stage of tumor development remains largely unknown. Here, we investigated the role of CAFs in facilitating the initial events of cancer metastasis when primary tumors were at microscopic sizes.

Experimental Design: Multicolor-coded cancer cells and CAFs were coimplanted into the transparent zebrafish body and metastasis at a single-cell level was monitored in living animals. Healthy fibroblasts, tumor factor–educated fibroblasts, and CAFs isolated from various tumors were tested for their ability to facilitate metastasis.

Results: We showed that CAFs promoted cancer cell metastasis at the very early stage during primary tumor development. When a primary tumor was at the microscopic size consisting of a few hundred cells, CAFs were able to hijack cancer cells for dissemination from the primary site. Surprisingly, a majority of metastatic cancer cells remained in tight association with CAFs in the circulation. Furthermore, stimulation of non–metastasis-promoting normal fibroblasts with TGF-B, FGF-2, HGF, and PDGF-BB led to acquisition of their metastatic capacity.

Conclusions: Cancer metastasis occurs at the very early stage of tumor formation consisting of only a few hundred cells. CAFs are the key cellular determinant for metastasis. Our findings provide novel mechanistic insights on CAFs in promoting cancer metastasis and targeting CAFs for cancer therapy should be aimed at the early stage during cancer development. *Clin Cancer Res; 23(16); 4769–79. ©2017 AACR.*

Introduction

Tumor tissues contain diverse cell populations that relentlessly communicate with each other in the tumor microenvironment (TME; refs. 1–5). In addition to cancer cells, infiltration of other cellular components including vascular cells, inflammatory cells, fibroblasts, and other immune cells significantly contributes to tumor growth, invasion, and metastasis (1–5). CAFs often represent an irreversibly activated fibroblast population that expresses alpha-smooth muscle actin (α-SMA; refs. 6–8). Once activated, CAFs produce various molecular signaling molecules to facilitate cancer growth and invasion. In addition, CAFs communicate with other nonmalignant cellular components including vascular and inflammatory cells to execute their multifunctions in modulation of tumor growth and invasion. For example, activated CAFs produce inflammatory cytokines and angiogenic factors to indirectly modulate tumor growth and metastasis (8). Metastasis is the major cause of mortality in cancer patients and occurs often at the early stage during cancer development (9, 10). Cancer metastasis is a complex process involving intravasation, extravasation, formation of the initial metastatic niche, and regrowth of metastatic nodules (10). A clinically detectable metastatic mass often represents the endpoint of the metastatic cascade. Advanced imaging technologies for early detection of tiny metastatic masses, especially microscopic cancer nodules, are not available. While it is known that most cancers possess the intrinsic features for metastasis, the exact events of cancer cell dissemination from the primary site and intravasation into the circulation are not known. In particular, it is unknown if metastasis already occurs when primary tumors are in tiny sizes.

Owing to their transparent and immunoprivileged features, developing zebrafish offers an outstanding opportunity to study single cancer cell behaviors from human and other species origins (11). Particularly, advanced imaging technologies have made it plausible for reconstitution of the TME with the multicolor-coded

[1]Department of Microbiology, Tumor and Cell Biology, Karolinska Institute, Stockholm, Sweden. [2]Jinan Infectious Disease Hospital, Shandong University, Jinan, China. [3]Department of Thyroid and Breast Surgery, the First Affiliated Hospital of Sun Yat-sen University, Guangzhou, China. [4]Key Laboratory of International Collaborations, Shenzhen Second People's Hospital, First Affiliated Hospital of Shenzhen University, Shenzhen, China. [5]Department of Oncology-Pathology, Karolinska Institute, Stockholm, Sweden. [6]Department of Medical and Health Sciences, Unit of Cardiovascular Medicine, Linköping University, Linköping, Sweden. [7]Department of Pathology and Department of Urology, the Affiliated Hospital of Qingdao University, Qingdao, China.

Note: Supplementary data for this article are available at Clinical Cancer Research Online (http://clincancerres.aacrjournals.org/).

C. Liu and Y. Zhang contributed equally to this article.

Corresponding Authors: Yihai Cao, Karolinska Institutet, Nobels väg 16, Stockholm 171 77, Sweden. Phone: +468-5248-7596; Fax: +468-33-13-99; E-mail: yihai.cao@ki.se; and Guohui Nie, Shenzhen Second People's Hospital, 3002 Sungang W Rd, Futian Qu, Shenzhen Shi, Guangdong Sheng 518029, China. E-mail: hghui2017@163.com

doi: 10.1158/1078-0432.CCR-17-0101

Translational Relevance

Understanding molecular mechanisms that underlie cancer metastasis is essential for development of novel therapeutics. Our findings indicate that activated CAFs can hijack noninvasive cancer cells to remote tissues and organs. Thus, the composition and activation status of CAFs, but not necessarily malignant cells *per se*, are the key determinants for cancer metastasis. Invasive assessment of CAFs isolated from the patient tumor tissue biopsies in our novel zebrafish model would provide crucial information for prognostication. This functional assay is complementary to the existing histopathologic diagnosis in the clinic. Additionally, targeting CAF signaling pathways as shown a few examples in our study would provide an effective therapy for treatment of cancer metastasis. Thus, our findings are highly relevant to cancer diagnosis, prognosis and therapy.

diverse cell populations (11). The color-coded TME reconstitution in zebrafish would allow us directly visualize single cancer cell migration, interaction with other host cells, metastatic intravasation, and extravasation in a living fish body. Particularly, this metastatic model provides a unique opportunity to study cancer metastasis at the early stage during cancer development. In this study, we showed that CAFs were a crucial cellular component in TME for promoting cancer metastasis. In several cancer models, we provided compelling evidence to demonstrate that CAFs but not normal fibroblasts promote cancer cell metastasis when primary tumors were at microscopic sizes. Moreover, metastatic cancer cells remained tightly associated with CAFs, supporting the essential role of CAFs for subsequent extravasation and the metastatic niche formation. Unraveling mechanisms underlying CAFs in cancer metastasis has conceptual and clinical implications for cancer therapy.

Materials and Methods

Zebrafish tumor model

All animal experiments were approved by the Northern Stockholm Experimental Animal Ethical Committee. Zebrafish embryos of the transgenic strain expressing enhanced GFP under the fli1 promoter (*Fli1:EGFP*; ref. 12) were raised at 28°C under standard experimental conditions. Zebrafish embryos at the age of 24 hpf were incubated in aquarium water containing 0.2 mmol/L 1-phenyl-2-thio-urea (PTU, Sigma). At 48-hpf, *Fli1:EGFP* zebrafish embryos were dechorionated with a pair of sharp-tip forceps and anesthetized with 0.04 mg/mL of tricaine (MS-222, Sigma). Anesthetized embryos were subjected for microinjection. Various tumor cells and fibroblasts were labeled *in vitro* with 2 μg/mL of 1,1′-Dioctadecyl-3,3,3′,3′- tetramethylindocarbocyanine perchlorate (DiI, Sigma) or a Vybrant DiD cell-labeling solution (Life Technologies), respectively. Approximately 500 tumor cells or a mixture consisting of 300 cancer cells and 200 fibroblasts were resuspended in DMEM (Hyclone) and 5 nL of the cell solution were injected into the perivitelline space (PVS) of each embryo by an Eppendorf microinjector (FemtoJet 5247, Eppendorf and Manipulator MM33-Right, Märzhäuser Wetziar). Non-filamentous borosilicate glass capillaries needles were used for injection and the injected zebrafish embryos were immediately transferred into PTU aquarium water. Zebrafish embryos were monitored 72 hours for investigating tumor invasion and metastasis using a fluorescent microscope (Nikon Eclipse C1).

Primary cell lines

Cancer cells and fibroblasts used in this study included human HuH7 hepatocellular carcinoma cells (HCC; ATCC); human A549 lung adenocarcinoma epithelial cells (NSCLC; kindly provided by Dr. Tatiana Pavlova, the Karolinska Institute, Sweden); human A431 squamous carcinoma cells (kindly provided by Dr. Keiko Funa, Gothenburg University, Sweden); human MiaPaCa-2 pancreatic ductal adenocarcinoma cells (PDAC; catalog no. FS0095, ATCC); human MDA-MB-231 breast cancer cells (ATCC HTB-26); human SW480 colon cancer cells (ATCC catalog no. ab01589); mouse MC38 colon adenocarcinoma cells (CRC; kindly provided by Dr. Ruben Hernandez, University of Navarra, Pamplona, Spain); murine E0771 breast cancer cells (catalog no. 940001, CH3 BioSystems); normal human prostate fibroblasts (NF;catalog no. P10893, Innoprot); human colorectal cancer (CRC)–derived CAFs (Isolated from a human colorectal cancer, kindly provided by Dr. Johan Hartman at the Department of Oncology-Pathology, Karolinska Institutet, Stockholm, Sweden); human prostate cancer–derived CAFs (PC-CAFs, catalog no. 159366A1, Asternad); and mouse cancer-derived CAFs (isolated from a T241 tumor). T241 tumors grown in GFP-transgenic mice were cut into small pieces and digested at 37°C for 60 minutes in a solution containing 0.15% collagenases I and II. After PBS washing, cells were filtered through a 40-μm cell strainer and were centrifuged at 1,500 rpm for 10 minutes. Single cells were stained with a rat anti-mouse CD31 antibody (1:100; catalog No. 553370, BD-Pharmingen) for 45 minutes, followed by incubation on ice for 20 minutes with an Alexa Fluor 555–labeled goat anti-rat antibody. GFP^- and GFP^+ cell populations were analyzed and sorted by FACS (MoFlo XTD, Beckman Coulter) and were cultured in 10% FBS-DMEM. Cells less than 10 passages were used through experiments. HuH7, A431, MiaPaCa-2, MDA-MB-231, and MC38 cancer cells were grown in 10% FBS-DMEM. E0771 cells were grown in 10% FBS-RPMI-1640 medium. A549 cells were grown in 10% FBS-IMEM. Human normal fibroblasts and CAFs were grown in a Fibroblast Medium Kit (catalog no. P60108, Innoprot), supplemented with 10% FBS. All cell lines were not authenticated after purchase or transferred from other laboratories but were routinely tested negative for *mycoplasma* by using the Mycoplasma Detection Kit (Lonza Inc.). HGF was purchased from the R&D Systems Inc., PDGF-BB was purchased from the PeproTech, FGF-2 was purchased from the Phamacia & UpJohn, and TGFβ-1 was purchased from the Thermo Fisher (catalog no. RP 39357).

CAF isolation

Fresh human colon cancer tissues were provided from the Karolinska University Hospital, and all tissue studies and handling were approved by the Stockholm Regional Ethical Committee (Ethical number 2016/957-31). Patient samples were transferred to research laboratories anonymously. Fresh cancer samples were washed with serum-free DMEM, cut into small pieces, and were transferred to a 0.15% collagenase IV solution, followed by incubation at 37°C for 40 minutes. Digested cells were filtered through a 40-mm cell strainer (BD Biosciences) and centrifuged at 1,500 rpm for 10 minutes. The single-cell suspension was incubated in a Fibroblast Medium Kit (catalog No. P60108, Innoprot) for 24 hours, allowing fibroblasts to attach

on culture plates. Unattached cells were removed after 24-hour incubation, and the adherent cells were further cultivated for experiments. Isolated fibroblasts from tumor tissues were defined as CAFs. This method yielded a relatively pure population of fibroblasts. Cultured CAFs less than five passages were used for our experiments.

Cell motility assay

DiI-labeled HuH7 single-cell suspension at the density of 2.5×10^4 cells/mL was mixed at a 3:1 ratio with normal fibroblasts or CAFs. A same number of tumor cells were used as a control. Mixed and unmixed cells were transferred onto a 12-well plate with flat bottom (Corning, Costar 12-well cell culture plate, Sigma Aldrich, catalog No.CLS3513) and were cultured for 24 hours. After confluency of monolayers, a sterile razor blade was used to create a uniformed cell-free wound of 0.5×1.0 cm on each well. The plates were washed 3 times with PBS to remove floating cells. Bright-field and fluorescent pictures were taken immediately after scratch (0 hour). Cells were cultured for 48 hours with 2% FBS-DMEM containing HuH7 alone or mixed cells with 2% FBS-IMDM and 2% FBS-DMEM. Cells were photographed and migrating cancer cells were counted manually using a Photoshop CS5 software program.

Matrigel invasion assay

Matrigel invasion assay was performed as previously described (13). Single-cell suspension of DiI-labeled HuH7 tumor cells, fibroblasts, or CAFs (2×10^4 cells/mL) were prepared in 10% FBS-DMEM. Tumor cells were mixed with fibroblasts, or CAFs at a 1:1 ratio and cell mixtures were transferred to a low adhesive 96-well plate with rounded bottom (Nunc low cell binding MicroWell plate; catalog no. Z721093-8EA, Sigma), followed by 24-hour coculture. Sphere-containing medium (50 μL) was mixed with 100 μL of Matrigel in each of 96-well plate. Bright-field and fluorescent pictures were taken immediately (0 hour). Cells were cultured for 48 hours with 2% FBS-DMEM containing HuH7 alone or mixed cells with 2% FBS-IMDM and 2% FBS-DMEM. Cells were photographed and migrating cancer cells were counted manually using a Photoshop CS5 software program.

Histology and IHC

Paraffin-embedded tissue sections in 5-mm thickness were stained with hematoxylin and eosin (H&E) using our standard protocols (10, 13–27). For α-SMA and FSP1 staining, the paraffin-embedded tissue sections were incubated at 4°C overnight using a mouse anti-human α-SMA antibody (1:4; catalog no. Clone 1A4 Dako) mixed with a rabbit anti-human/mouse FSP1 antibody (1:200, catalog no. 07-2274, Millipore). A mixture of secondary antibodies comprising an Alexa Fluor 555-labeled goat anti-mouse antibody (1:200; Invitrogen) and an Alexa Fluor 488-labeled donkey anti-rabbit antibody (1:200; Invitrogen) was used. Paraffin-embedded tissue sections were incubated at 4°C overnight with a goat anti-human/mouse desmin antibody (1:200; catalog no. AF3844, R&D Systems) mixed with a rabbit anti-human/mouse PDGFRα antibody (1:200; catalog no. 3164, Cell Signaling Technology). A mixture of secondary antibodies comprising an Alexa Fluor 555-labeled goat anti-mouse antibody (1:200; Invitrogen) and an Alexa Fluor 488-labeled donkey anti-rabbit antibody (1:200; Invitrogen) was used. Positive signals were captured using a fluorescence microscope equipped with a Nikon DS-QilMC camera (Nikon Corporation).

Immunocytochemistry

For α-SMA and PDGFRα staining, the fixed CAFs and NFs were incubated at 4°C overnight using a mouse anti-human α-SMA antibody (1:4; catalog no. Clone 1A4, Dako) mixed with a rabbit anti-human/mouse PDGFRα antibody (1:200; catalog no. 3164, Cell Signaling Technology), followed by staining with a mixture of secondary antibodies comprising an Alexa Fluor 555-labeled goat anti-mouse antibody (1:200; Invitrogen) and an Alexa Fluor 488-labeled donkey anti-rabbit antibody (1:200; Invitrogen). For desmin and FSP1 staining, the fixed CAFs and NFs were incubated at 4°C overnight with a goat anti-human desmin antibody (1:200; catalog no AF3844, R&D Systems) mixed with a rabbit anti-human/mouse FSP1 antibody (1:200, catalog no. 07-2274, Millipore). A mixture of secondary antibodies comprising an Alexa Fluor 555-labeled goat anti-mouse antibody (1:200; Invitrogen) and an Alexa Fluor 488-labeled donkey anti-rabbit antibody (1:200; Invitrogen) was used. Positive signals were captured using a fluorescence microscope equipped with a Nikon DS-QilMC camera (Nikon Corporation).

qPCR

Quantitative PCR (qPCR) was performed according to a standard protocol (28). In brief, total RNA samples were prepared by a GeneJet RNA Purification Kit (catalog no. K0731, Thermo Scientific) and a cDNA Synthesis Kit (catalog no. K1632, Thermo Scientific). A Power SYBR Green Master Mix Kit (catalog no. 4367659, Applied Biosystems) and a Step One Plus real-time PCR system (Applied Biosystems) were applied. The following paired primers were used: human *Gapdh* forward: 5′-CCAGCAAGGACACTGAGCAA-3′ and human *Gapdh* reverse: 5′-GGGATGGAAATTGTGAGGGA-3′; human *α-Sma* forward: 5′-AGGGGGTGATGGTGGGAATG-3′ and human *α-Sma* reverse: 5′-GCCCATCAGGCAACTCGTAAC-3′; human *Fap* forward: 5′-GCTAACTTTCAAAAACATCTGGAAAAATG-3′ and human *Fap* reverse: 5′-GTAATATGTTGCTGTGTAAGAGTATCTCC-3′; mouse *Ccl5* forward 5′- GCTGCTTTGCCTACCTCTCC-3′ and mouse *Ccl5* reverse 5′-TCGAGTGACAAACACGACTGC-3′; mouse *Cxcl12* forward 5′-TGCATCAGTGACGGTAAACCA-3′ and mouse *Cxcl12* reverse 5′-TTCTTCAGCCGTGCAACAATC-3′; mouse *Il33* forward 5′-ATGGGAAGAAGCTCATGCTG-3′ and mouse *Il33* reverse 5′-CCGACGACTTTTTCTGAAGG-3′; mouse *Il1rl1* forward 5′-ATTCAGGGGACCATCAAGTG-3′ and mouse *Il1rl1* reverse 5′-CGTCTTGGAGGCTCTTTCTG-3′; mouse *Gapdh* forward 5′-CCAGCAAGGACACTGAGCAA-3′ and mouse *Gapdh* reverse 5′- GGGATGGAAATTGTGAGGGA-3′.

Stimulation of fibroblasts

FGF-2 (10 ng/mL), HGF (10 ng/mL), PDGF-BB (10 ng/mL), and TGFβ-1 (10 ng/mL) were used to stimulate the fibroblasts for 24 hours. The growth factor–stimulated fibroblasts together with HCC or NSCLC cells were coinjected into the perivitelline space of each zebrafish embryo using the same method described above.

Affymetrix gene array

Mouse stromal cells were treated with or without 100 ng/mL PDGF-BB for 72 hours and total RNA was extracted with an RNA extraction kit (Thermo Fisher Scientific). Samples (triplicates per group) were used for the gene expression-profiling analyses. Normalization and analysis for differentially expressed genes were performed using robust multi-array analysis and significance

analysis of microarrays (SAM) through the R statistical software packages, oligo and samr. Heatmaps were presented for up- and downregulation of gene expression using the Multiple Experiment Viewer system (version 4.7). Gene array data were deposited in the Gene Expression Omnibus, accession number GSE33717.

Statistical analysis

Statistical analysis was performed using the standard Student *t* test for pair comparisons and ANOVA analysis for multiple factors. Data were presented as means of determinants (±SEM) and *P* values of *, $P < 0.05$; **, $P < 0.01$; ***, $P < 0.001$ were deemed as statistically significant, very significant, and extremely significant, respectively.

Results

Tumor fibrosis and isolation of human CAFs

To study the role of CAFs in facilitating cancer invasion at the initial steps of the metastatic cascade, we developed a zebrafish cancer model in which different cell populations in the TME can be visualized by color codes. Solid tumors contain high proportions of a fibrotic component that is often associated with an invasive and metastatic phenotype. To visualize the fibrotic component in human tumors, we defined CAFs in a freshly dissected human colorectal cancer (CRC) using several specific markers. H&E staining showed a high proportion of the fibrotic component in this invasive and metastatic tumor (Supplementary Fig. S1A). Immunohistochemical staining with fibroblast specific markers (15), including alpha-smooth muscle actin (α-SMA), fibroblast specific protein-1 (FSP-1), desmin, and PDGFRα, validated the existence of the high CAF content in this invasive CRC tumor (Supplementary Fig. S1A).

We next isolated and defined these CAFs and human normal fibroblasts for expression of FSP-1, desmin, and PDGFRα (Supplementary Fig. S1B). Interestingly, human normal fibroblasts only expressed a very low level of α-SMA (Supplemental Fig. 1B and C). These findings demonstrate that isolated CAFs were α-SMA^{+} myofibroblasts, which is known to be associated with cancer invasion. In contrast, human SW480 CRC cancer cells with an epithelial origin lacked detectable levels of fibrotic markers (Supplementary Fig. S1C and S1D). Together, these data show that primary CAFs isolated from a human CRC possess distinct marker features compared with healthy human fibroblasts.

CAFs promote cancer cell migration and invasion

We next investigated the functional properties of CAFs in cancer invasion using *in vitro* cancer cell migration and invasion assays. In a cell motility assay, a mixture of cancer cells and CAFs was cocultured at a 3:1 ratio for 48 hours, followed by creating a uniform wound. After 24 hours, migrating cancer cells in the wound area of each sample were counted. CAFs isolated from a human prostate cancer and isolated from a human CRC markedly promoted tumor cell migration (Fig. 1A and B). Normal human fibroblasts lacked the ability to facilitate cancer cell migration. In contrast, normal human fibroblasts significantly inhibited cancer cell migration in this *in vitro* assay (Fig. 1A and B).

To further study the functional features of CAFs in cancer invasion, we developed a Matrigel assay in which cancer cells and CAFs were mixed at a 1:1 ratio. Again, CAFs isolated from two independent tumor types, but not normal fibroblasts, markedly promoted cancer cell invasion (Fig. 1C and D). It appeared that CRC-CAFs exhibited more potent effects than PC-CAFs in promoting cancer invasion, perhaps reflecting the intrinsic invasive property of various cancers. These data demonstrate that CAFs promote cancer cell invasion in these *in vitro* assays.

CAF behavior in a zebrafish model

We recently developed a zebrafish model to study cancer metastasis, particularly to decipher the initial steps of the

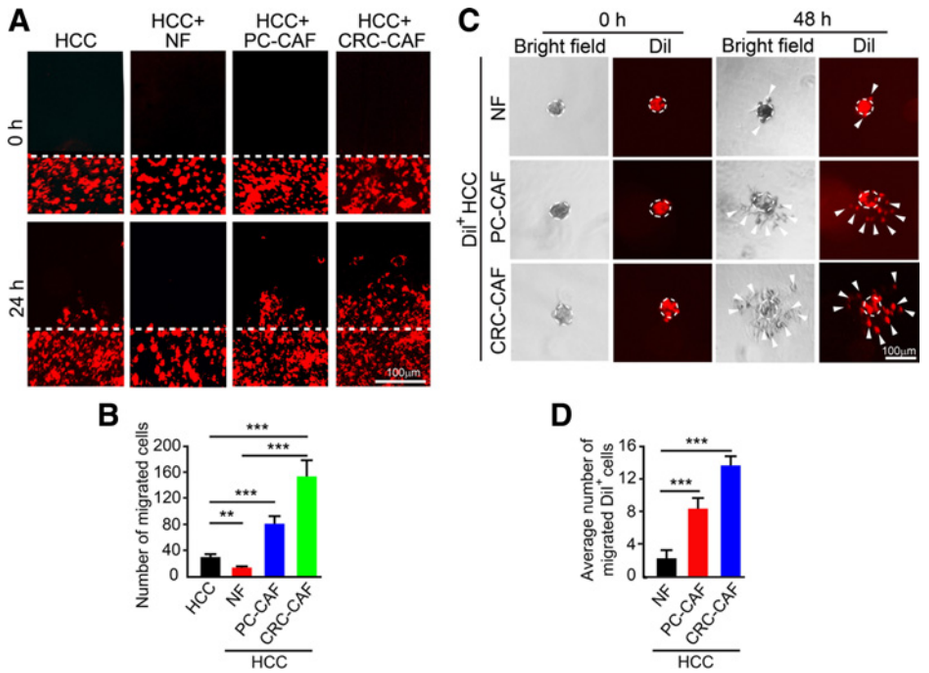

Figure 1.
Human HCC cancer cell migration and invasion in the presence of CAFs. **A,** Micrographs of HCC cell (red) migration in the presence of normal fibroblasts (NF), CAFs isolated from a human prostate cancer (PC-CAF), or CAFs isolated from a human CRC (CRC-CAF). Dashed lines mark the borders of the created wound in culture. **B,** Quantification of migrated cells beyond the wound areas ($n = 5$ samples/group). **C,** Micrographs of HCC invasion in a Matrigel assay in the presence of CRC-CAFs, PC-CAFs, or normal fibroblasts (NF). Dashed lines encircle the original cell spheres. Arrowheads indicate invasive tumor cells (red). **D,** Quantification of invasive cells ($n = 5$ samples/group). **, $P < 0.01$; ***, $P < 0.001$ (mean ± SEM, Student *t* test).

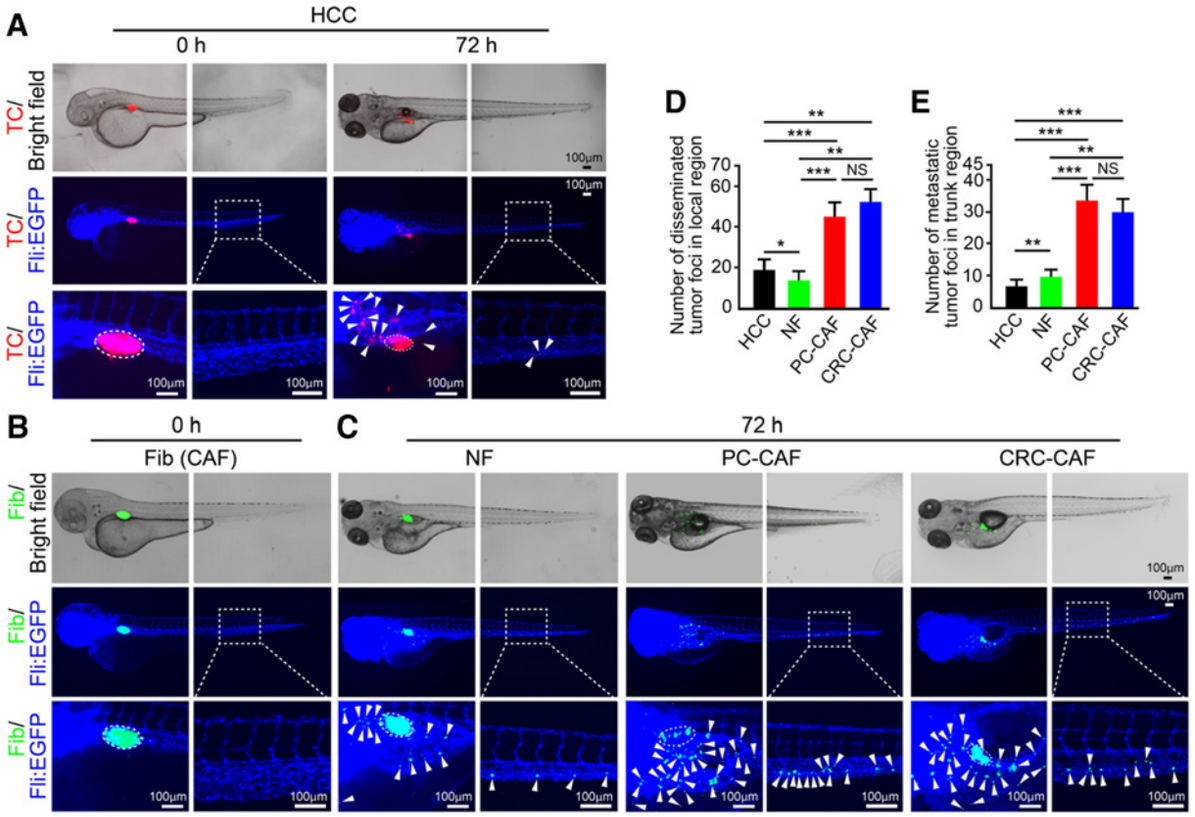

Figure 2.

Dissemination of CAFs and cancer cells. **A–C,** Micrographs HCC-alone implanted (red; **A**), normal fibroblast-alone implanted (green), PC-CAF–alone implanted (green), and CRC-CAF–alone implanted (green) zebrafish. Blood vasculatures are shown in blue. Dashed circles indicate the primary tumor areas. Dashed squares amplify the indicated regions. Arrowheads point to disseminated and metastatic tumor cells or fibroblasts. **D** and **E,** Quantification of the total numbers of disseminated and metastatic cells in the primary tumor surroundings and in the trunk regions of zebrafish (HCC, $n = 10$ zebrafish/group; NF, $n = 11$ zebrafish/group; PC-CAF, $n = 17$ zebrafish/group; CRC-CAF, $n = 7$ zebrafish/group). **, $P < 0.01$; ***, $P < 0.001$ (mean ± SEM, Student t test). NS, not significant.

metastatic cascade, which remains a challenging issue in other animal models such as in rodent cancer models. The transparent and immune-privileged nature of zebrafish embryos allowed us to monitor human or mouse tumor cell migration and metastasis in the living fish body even when primary tumors were at microscopic sizes. Approximately 500 DiI-red–labeled human HCC cells were injected into the perivitelline space of each zebrafish embryo. Tumor cell invasion and metastasis in the zebrafish body were monitored at 72 hours postinjection. Injection of HCC cells alone resulted in dissemination of tumor cells from the original primary tumor sites (Fig. 2A). However, only a limited number of cancer cells were detectable at the surrounding regions of primary tumors and metastatic tumor cells were rarely found in distal regions such as the trunk region of the zebrafish embryo (Fig. 2A and D).

To study behaviors of CAFs in the zebrafish body, CAFs, shown in green, were labeled with DiD dye and 500 CAF cells were implanted into the perivitelline space of each zebrafish embryo. Surprisingly, CRC-CAFs and PC-CAFs were highly "metastatic" and substantial numbers of CAFs were disseminated to distal regions of the zebrafish body (Fig. 2B–E). These findings show that CAFs were highly motile and "metastatic" in the zebrafish body.

CAF promotes the initial events of cancer metastasis

To study the role of CAFs in facilitating cancer metastasis in TME, we developed a zebrafish model in which different color-coded CAFs and cancer cells were coimplanted into the zebrafish body (Fig. 3A; ref. 11). Implantation of HCC tumor cells alone resulted in a modest effect of cancer metastasis (Fig. 3B, D, and E). Coimplantation of HCC cells with normal human fibroblasts significantly reduced the number of metastatic cancer cells (Fig. 3C–E), suggesting that the healthy fibroblasts might inhibit cancer cell motility and metastasis. However, coimplantation of CRC-CAFs and PC-CAFs with cancer cells markedly increased the number of metastatic cells in different parts of the zebrafish body (Fig. 3C–E). The disseminated tumor cells were visible in the head and trunk regions of the zebrafish body. Quantification analysis showed that the number of distal metastatic tumor cells was markedly higher in CRC-CAF-HCC- and PC-CAF-HCC-coimplanted zebrafish (Fig. 3F). Surprisingly, most distal metastatic cancer cells were associated with CAFs that showed double color positivity (Fig. 3C). Approximately, 80% of the distal metastatic cancer cells were associated with CAFs (Fig. 3F and G). These findings provide compelling evidence that CAFs facilitate cancer cell metastasis and the intimate interactions between cancer cells and CAFs remain even after the intravasation event.

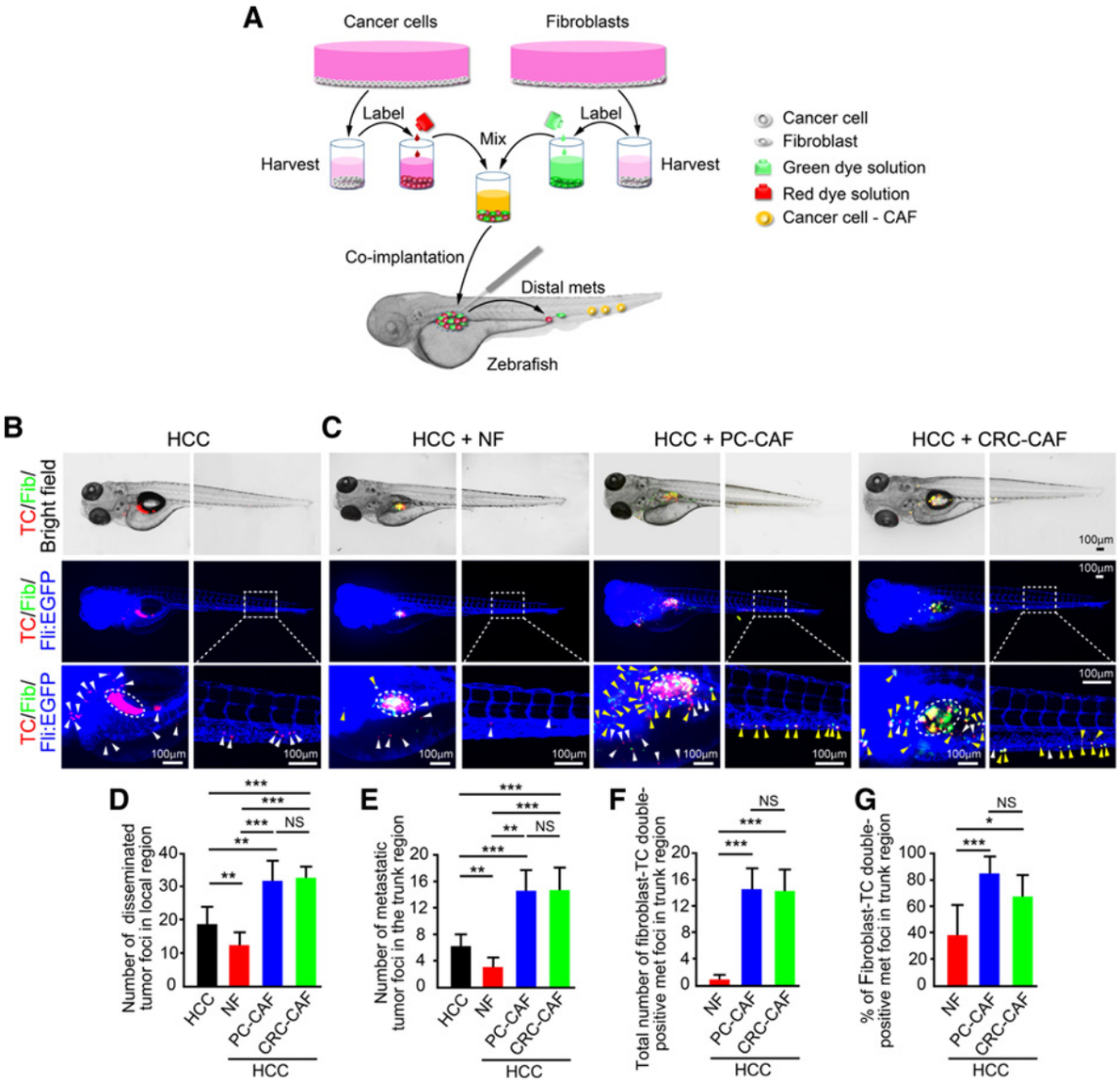

Figure 3.

CAFs promote liver cancer metastasis. **A,** Schematic diagram of coimplantation of cancer cells and fibroblasts. Cultured monolayers of cancer cells, fibroblasts, and CAFs were harvested and labeled with different colors. The labeled cells were mixed and coimplanted into the perivitelline space of each zebrafish. Dissemination of cancer cells, CAFs, and the cancer cell–CAF complex was monitored. **B** and **C,** Micrographs of HCC-alone implanted (red), HCC plus normal fibroblasts (green), HCC plus PC-CAFs (green), and HCC plus CRC-CAFs (green) were implanted into the perivitelline space of each zebrafish. After 72 hours postimplantation, dissemination of implanted cells was monitored. White arrowheads point to disseminated and metastatic cancer cells, yellow arrowheads point to overlapping cancer cells and fibroblasts. **D** and **E,** Quantification of total numbers of disseminated and metastatic cells in the primary tumor surroundings and in the trunk regions of zebrafish (HCC, $n = 10$ samples per group; NF + HCC, $n = 11$ samples per group; HCC + PC-CAF, $n = 15$ samples per group; HCC + CRC-CAF, $n = 11$ samples per group). **F** and **G,** Quantification of HCC-fibroblast double-positive metastatic foci in the trunk regions of zebrafish (HCC, $n = 10$ samples per group; HCC+NF, $n = 11$ samples per group; HCC + PC-CAF, $n = 15$ samples per group; HCC + CRC-CAF, $n = 11$ samples per group). *, $P < 0.05$; **, $P < 0.01$; ***, $P < 0.001$ (mean ± SEM, Student t test). NS, not significant.

To further validate these findings, we performed similar experiments with a human lung cancer cell line (A549 NSCLC). The metastasis-promoting effect of CAFs was further validated in this cancer model (Fig. 4). Again, a majority of metastatic cancer cells remained association with CAFs. Similar data were also obtained from other tumor models including squamous carcinoma, pancreatic ductal adenocarcinoma (PDAC), and breast cancer, showing that CFAs markedly promoted cancer metastasis (Fig. 5). We also provided compelling evidence showing that mouse CAFs isolated from a fibrosarcoma also markedly promoted mouse breast cancer and CRC cancer metastasis (Supplementary Figs. S2 and S3). A video clip showed dissemination of CAF-cancer cell complex from the original tumor site (Video 1). Together, several independent cancer models demonstrate that CAFs display

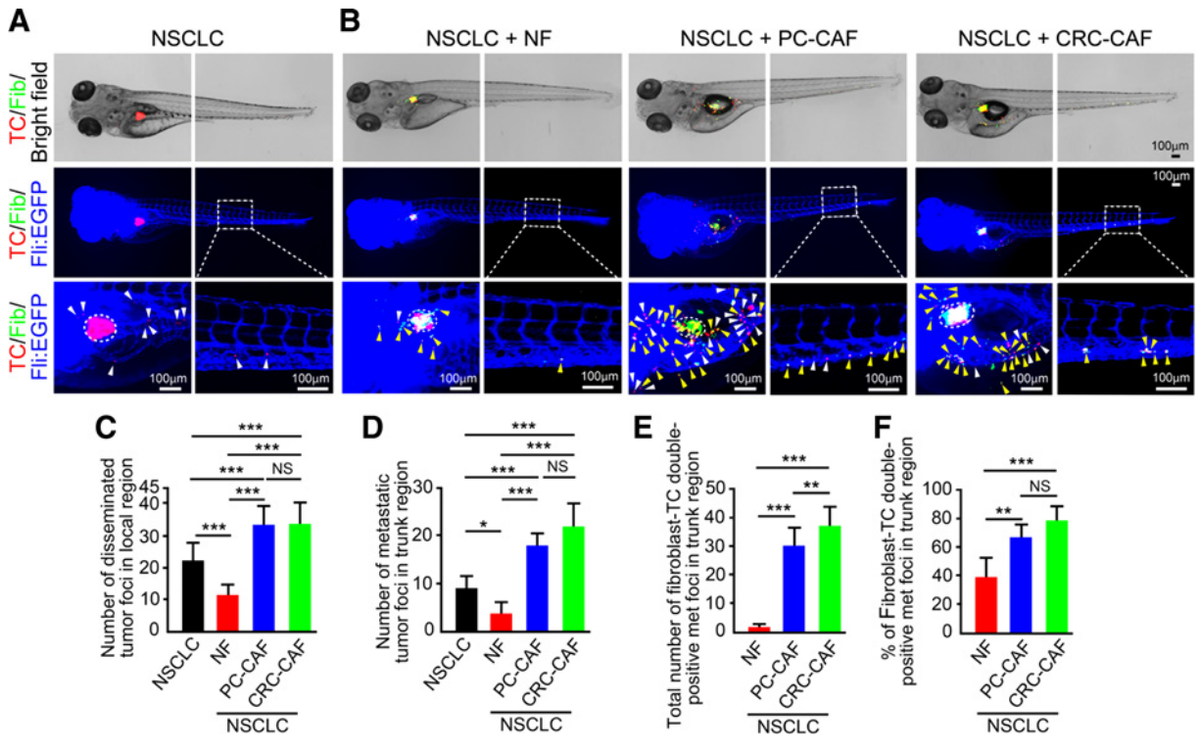

Figure 4.

CAFs promote lung cancer metastasis. **A** and **B,** Micrographs of NSCLC-alone implanted (red), NSCLC plus normal fibroblasts (green), NSCLC plus PC-CAFs (green), and NSCLC plus CRC-CAFs (green) that were implanted into the perivitelline space of each zebrafish. After 72 hours postimplantation, dissemination of implanted cells was monitored. White arrowheads point to disseminated and metastatic cancer cells, yellow arrowheads point to overlapping cancer cells and fibroblasts. **C** and **D,** Quantification of total number of disseminated and metastatic cells in the local primary tumor surroundings and trunk regions of zebrafish (NSCLC, $n = 10$ samples per group; NF + NSCLC, $n = 10$ samples per group; NSCLC + PC-CAF, $n = 7$ samples per group; NSCLC + CRC-CAF, $n = 8$ samples per group). **E** and **F,** Quantification of NSCLC-fibroblast double-positive metastatic foci in the trunk regions of zebrafish (NSCLC, $n = 10$ samples per group; NSCLC+NF, $n = 10$ samples per group; NSCLC + PC-CAF, $n = 7$ samples per group; NSCLC + CRC-CAF, $n = 8$ samples per group). *, $P < 0.05$; **, $P < 0.01$; ***, $P < 0.001$ (mean ± SEM, Student t test). NS, not significant.

marked effects in promoting metastasis and remained in close association with metastatic cancer cells in distal tissues.

Growth factor–stimulated fibroblasts promote cancer metastasis

Knowing that the normal healthy fibroblasts lacked the ability for promoting cancer metastasis, we next stimulated these cells with growth factors targeting fibroblasts. It is known that fibroblasts are target cells for fibroblast growth factor-2 (FGF-2), hepatocyte growth factor (HGF), platelet-derived growth factor–BB (PDGF-BB), and transforming growth factor-beta 1 (TGFβ-1; ref. 6). Therefore, we stimulated the normal healthy fibroblasts with FGF-2, HGF, PDGF-BB, and TGFβ-1 and the stimulated fibroblasts were subsequently coimplanted into the perivitelline space of each zebrafish. Interestingly, FGF-2–stimulated fibroblasts markedly promoted HCC metastasis (Fig. 6). Similarly, HGF-, PDGF-BB-, TGF β-1–stimulated normal fibroblasts also significantly promoted HCC cancer metastasis (Fig. 6). We provide independent evidence demonstrating that HGF, PDGF-BB, TGFβ-1 stimulated–normal fibroblasts considerably promoted NSCLC cancer metastasis (Supplementary Fig. S4). These findings provide new mechanistic insights on fibroblast-stimulating factors in promoting cancer metastasis.

Profiling of metastasis-related genes

To further gain mechanistic insights on fibroblast-mediated metastasis, we analyzed molecular signaling components that are known to be involved metastasis. Knowing PDGF-BB–stimulated fibroblasts were able to promote metastasis, we have focused our efforts on studying molecular changes of the PDGF-BB–stimulated fibroblasts. Metastasis-related genes including CCLs, CCRs, CXCLs, CXCRs, ILs, ILRs, and MMPs were particularly investigated. CCLs, including CCL5, CCL2, and CCL7, were upregulated, whereas CCL9, CXCL12, and CXCL14 were downregulated (Fig. 6G and H). Interestingly, IL-33 and its receptor ST2 (*Il1rl1*) were markedly upregulated (Fig. 6 and Supplementary Fig. S5). These data suggest that complex molecular mechanisms may be involved in mediating fibroblast-stimulated cancer metastasis.

Discussion

In this work, we provide novel mechanistic insights on CAFs in facilitating cancer metastasis. In the presence of CAFs, dissemination of cancer cells from the primary site to distal organs occurs at the early stage during cancer development. If these findings are successfully translated to clinical situations in cancer patients, they imply that tumors at microscopic size containing only a few

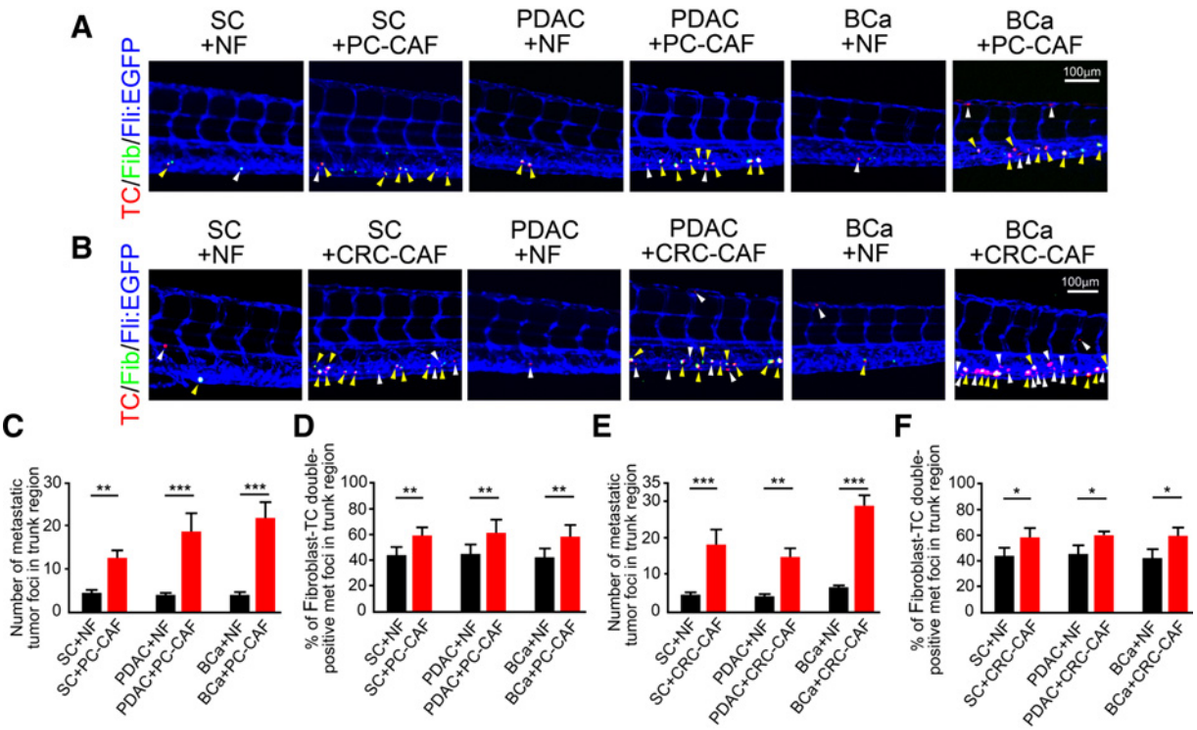

Figure 5.

CAFs promote metastasis of squamous carcinoma, pancreatic cancer, and breast cancer. **A** and **B,** Micrographs of the trunk regions of zebrafish with metastatic squamous carcinoma cells (SC) plus normal fibroblast (NF), squamous carcinoma (SC) plus PC-CAF, or SC plus CRC-CAF; PDAC plus NF, PDAC plus PC-CAF, or PDAC plus CRC-CAF; breast cancer cells (BCa) plus NF, BCa plus PC-CAF, and plus CRC-CAF. Cancer cells were labeled with red color, and NFs or CAFs were labeled with green color. After 72 hours postimplantation, dissemination of implanted cells was monitored. White arrowheads point to disseminated and metastatic cancer cells, yellow arrowheads point to overlapping cancer cells and fibroblasts. **C** and **E,** Quantification of total number of metastatic tumor foci in the trunk regions of zebrafish (SC + NF, $n = 13$ samples per group; SC + PC-CAF, $n = 6$ samples per group; SC + CRC-CAF, $n = 10$ samples per group; PDAC + NF, $n = 8$ samples per group; PDAC + PC-CAF, $n = 7$ samples per group; PDAC + CRC-CAF, $n = 4$ samples per group; BCa + NF, $n = 25$ samples per group; BCa + PC-CAF, $n = 6$ samples per group; BCa + CRC-CAF, $n = 16$ samples per group). **D** and **F,** The percentage of TC-fibroblast double-positive metastatic foci in the trunk regions of zebrafish (SC + NF, $n = 13$ samples per group; SC + PC-CAF, $n = 6$ samples per group; SC + CRC-CAF, $n = 10$ samples per group; PDAC + NF, $n = 8$ samples per group; PDAC + PC-CAF, $n = 7$ samples per group; PDAC + CRC-CAF, $n = 4$ samples per group; BCa + NF, $n = 25$ samples per group; BCa + PC-CAF, $n = 6$ samples per group; BCa + CRC-CAF, $n = 16$ samples per group). *, $P < 0.05$; **, $P < 0.01$; ***, $P < 0.001$ (mean ± SEM, Student t test).

hundred cells are already metastatic. At a microscopic size, the existence of a tiny tumor nodule in a given tissue or organ may not even be dependent on angiogenesis and cooption of the preexisting host vasculatures is sufficient for maintaining cancer cell survival (29, 30). Infiltration and activation of fibroblasts in these microscopic tumors are sufficient to promote cancer metastasis. If so, this may imply that cancer metastasis can occur in dormant tumors in which the primary tumor mass is not detectable and would not grow. Yet, these microscopic dormant tumors can cause serious troubles in cancer patients if fibroblasts become activated in tumors. Metastasis may also occur in microscopic avascular tumors in which tumor cells invade the preexisting surrounding blood vessels. Our zebrafish model provides compelling evidence to support this important concept. First, in the zebrafish model the implanted primary tumors remain similar sizes throughout the entire experimental duration. Thus, the growth-related tumor size is irrelevant to metastatic potentials. Second, the tiny microscopic tumor mass is not vascularized and dissemination of cancer cells is mediated through the preexisting surrounding host vasculatures. As various cellular components are color-coded, interactions of cancer cells and fibroblasts can be directly visualized at a single-cell level.

Our findings show that a majority of metastatic cancer cells in the circulation and distal tissues remain tightly associated with CAFs. These data imply that CAFs facilitate cancer metastasis at several distinct steps of the metastatic cascade. First, CAFs are crucially important for the initial intravasation of cancer cells into the circulation. In support of this notion, we show that CAFs are able to promote broad dissemination of cancer cells into the circulation. Secondly, the CAF–tumor cell complex, although lack of evidence, may be essential for extravasation to distal organs. Indeed, a recent study shows that fibroblasts and mesenchymal cells regulate cancer cell extravasation (31). This view was supported by several independent studies showing that metastatic cancer cells carry their fibrotic soil with them to distal organs (32–36). Thirdly, disseminated CAFs may promote the formation of initial metastatic niches and subsequent regrowth in distal tissues and organs. Thus, CAFs play dynamic roles in promoting cancer metastasis at different locations. One of the important issues underlying advantages of the CAF–tumor cell complex for dissemination is that the fibrotic cell type is the engine for promoting dissemination. Implantation of CAFs alone without cancer cells causes broad dissemination from the primary site supports the fact that CAFs enforce cancer cells moving away from

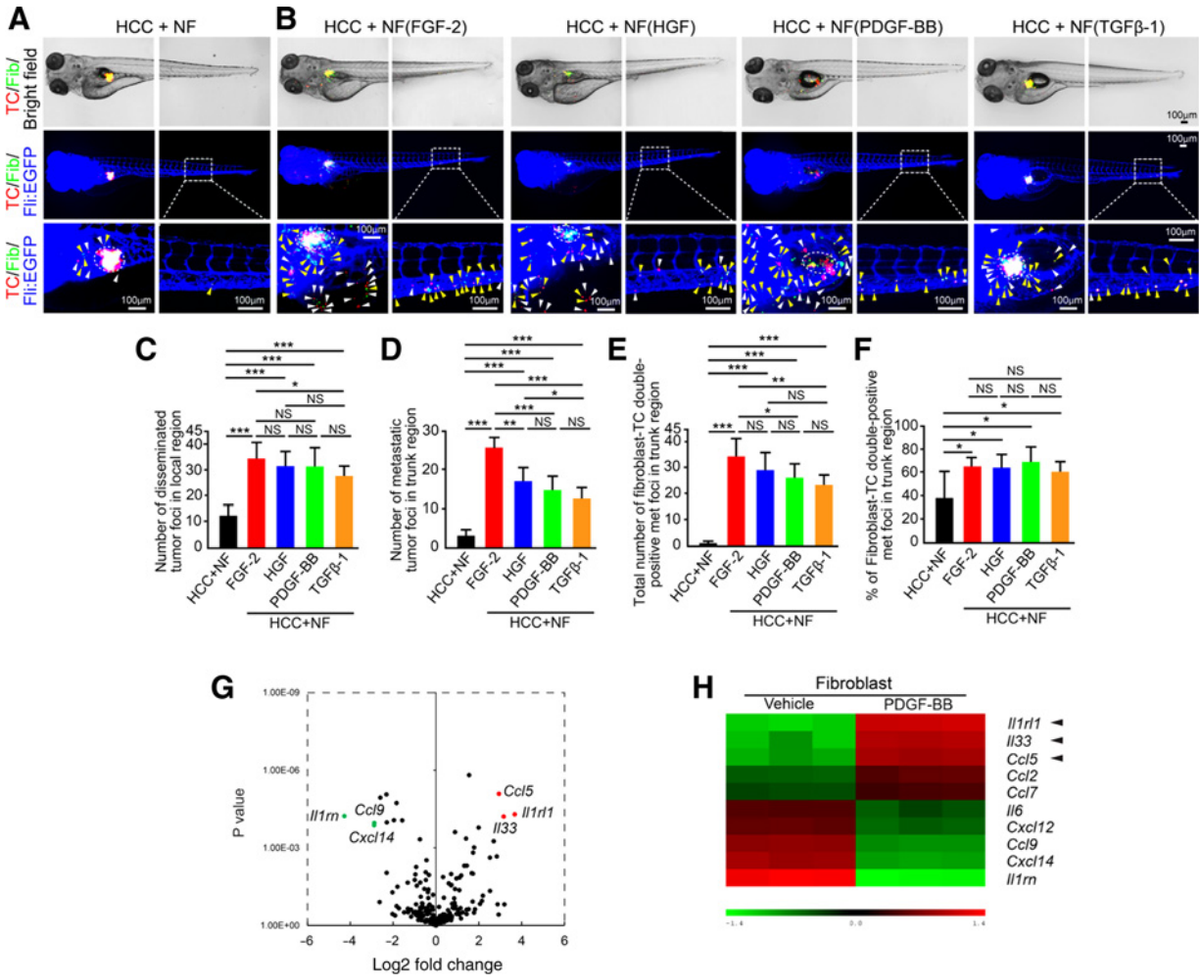

Figure 6.

Growth factor–stimulated fibroblasts promote HCC metastasis. **A** and **B,** Micrographs of zebrafish received coimplantation of HCC cells (red) and various growth factor–stimulated normal fibroblasts (NFs; green). White arrowheads point to disseminated and metastatic cancer cells, yellow arrowheads point to overlapping cancer cells and fibroblasts. **C–F,** Quantification of disseminated and metastatic cells in the local regions and trunk regions of zebrafish (HCC + NF, n =11 samples per group; HCC + NF-FGF-2, n = 14 samples per group; HCC + NF-HGF, n =12 samples per group; HCC + NF-PDGF-BB, n =8 samples per group; and HCC + NF-TGFβ-1, n = 10 samples per group). **G,** Volcano plot of metastasis-related genes by genome-wide expression profiling of PDGF-BB–stimulated fibroblasts (n = 3 samples per group). Top 3 most upregulated and downregulated genes are indicated. **H,** Heatmap of top 5 most up- and down-metastasis-related genes (n = 3 samples per group). *, $P < 0.05$; **, $P < 0.01$; ***, $P < 0.001$ (mean ± SEM, Student t test). NS, not significant.

their primary sites. Thus, our findings propose that the fibrotic soil carry the seeds, but not the seeds carrying soil, to distal tissues and organs. An extended view to clinical implications would be that targeting the fibrotic component in solid tumors is crucial for treatment of metastatic disease. Also, targeting fibroblasts at the early stage of cancer development is crucial for preventing metastasis. These important clinically related issues warrant further investigation.

Although in-depth molecular mechanisms underlying fibroblast-mediated cancer metastasis need to be elucidated, we can reasonably speculate several possibilities based on our findings. Of great interest, PDGF-BB–stimulated fibroblasts express high levels of IL-33 and its receptor ST2, which has been recently shown to promote cancer metastasis (13). Expression of both ligands and receptors in fibroblasts indicates the existence of an autocrine loop for fibroblast activation. Thus, the IL-33–ST2 pathway might be important for PDGF-BB–induced metastasis though activation of CAFs. Another interesting possibility is that PDGF-BB is able to promote myofibroblast formation, which is also crucial for induction of an invasive phenotype (15). The third possibility is that PDGF-BB induces chemokines particularly CCL5 that promotes cancer cell invasion and metastasis. It is known that CCL5 mediates breast cancer metastasis through a tumor stromal mechanism (37). Thus, sophisticated molecular mechanisms might be involved in fibroblast-mediated cancer metastasis. Perhaps, each fibroblast-stimulating factor, including members in the FGF, PDGF, TGF-β, and HGF families, uses different but yet overlapping mechanisms for promoting cancer metastasis. This interesting view warrants future studies.

Clinically, a frequently encountered situation is that the first sign of cancer disease is metastasis without overt primary tumors (38). In such a situation, the primary tumor may remain dormant

and avascular and is unable to grow into a detectable mass. However, tumor cells can be disseminated to the circulation and subsequently spread to various tissues and organs. In distal tissues and organs, owing to environmental changes, metastatic tumor cells can be vascularized and grow to a clinically detectable size. Perhaps, infiltration of CAFs in these microscopic tumors plays a determinant role in cancer metastasis. Indeed, metastasis occurs at the early stage of pancreatic ductal adenocarcinoma (PDAC) development and PDAC is one of the most fibrotic cancer types of all cancers. Also, the amount of the fibrotic component is reversely correlated with survival. In our experimental settings, a mixture of cancer cells and CAFs were cocultured at a 3:1 ratio, which is clinically relevant in some most common cancer types such as lung cancer and PDAC. Taken together, our present work provides a novel mechanistic insight into fibroblast-mediated cancer metastasis. Targeting the fibrotic compartment would be an important approach for cancer therapy.

Disclosure of Potential Conflicts of Interest

No potential conflicts of interest were disclosed.

Authors' Contributions

Conception and design: T. Alkasalias, Y. Cao
Development of methodology: Y. Yang, T. Pavlova, Y. Cao
Acquisition of data (provided animals, acquired and managed patients, provided facilities, etc.): S. Lim, T. Pavlova, T. Alkasalias, J. Hartman, Y. Cao, C. Liu, Y. Zhang
Analysis and interpretation of data (e.g., statistical analysis, biostatistics, computational analysis): S. Lim, Y. Yang, Y. Cao, C. Liu, Y. Zhang, K. Hosaka, X. Wang, Y. Lu, G. Nie
Writing, review, and/or revision of the manuscript: S. Lim, T. Alkasalias, J. Hartman, Y. Cao, C. Liu, Y. Zhang
Administrative, technical, or material support (i.e., reporting or organizing data, constructing databases): S. Lim, L. Jensen, X. Xing, Y. Cao
Study supervision: L. Jensen, Y. Cao

Grant Support

Y. Cao's laboratory is supported through research grants from the European Research Council (ERC) advanced grant ANGIOFAT (Project no 250021), the Swedish Research Council (K2012-67X-21130-04-5), the Swedish Cancer Foundation (140659), the Karolinska Institute Foundation (C166658073), the Karolinska Institute distinguished professor award (C166646352), the Torsten Soderbergs Foundation (M144/12), the Maud and Birger Gustavsson Foundation (C166655073), the NOVO Nordisk Foundation (BtN/AIR 2014), and the Knut and Alice Wallenbergs Foundation (C166646483). Tatiana Pavlova and Twana Alkasalias were supported by grants from the Swedish Research Council (2015-02410), the Swedish Cancer Society (15 0591) and Cancer Research Institute, New York (July 2016-June 2017). Guohui Nie is supported by Fund for High Level University Construction of Medical Discipline (2016031638), China.

The costs of publication of this article were defrayed in part by the payment of page charges. This article must therefore be hereby marked *advertisement* in accordance with 18 U.S.C. Section 1734 solely to indicate this fact.

Received January 12, 2017; revised February 14, 2017; accepted April 14, 2017; published OnlineFirst April 18, 2017.

References

1. Hanahan D, Weinberg RA. The hallmarks of cancer. Cell 2000;100:57–70.
2. McCarthy N. Tumour microenvironment: the same, but different. Nat Rev Cancer 2011;11:232.
3. Meads MB, Gatenby RA, Dalton WS. Environment-mediated drug resistance: a major contributor to minimal residual disease. Nat Rev Cancer 2009;9:665–74.
4. Joyce JA, Pollard JW. Microenvironmental regulation of metastasis. Nat Rev Cancer 2009;9:239–52.
5. Overall CM, Kleifeld O. Tumour microenvironment - opinion: validating matrix metalloproteinases as drug targets and anti-targets for cancer therapy. Nat Rev Cancer 2006;6:227–39.
6. Kalluri R. The biology and function of fibroblasts in cancer. Nat Rev Cancer 2016;16:582–98.
7. Seton-Rogers S. Pancreatic cancer: Fibroblast co-conspirators. Nat Rev Cancer 2011;11:758.
8. Kalluri R, Zeisberg M. Fibroblasts in cancer. Nat Rev Cancer 2006;6:392–401.
9. Lee SL, Rouhi P, Dahl Jensen L, Zhang D, Ji H, Hauptmann G, et al. Hypoxia-induced pathological angiogenesis mediates tumor cell dissemination, invasion, and metastasis in a zebrafish tumor model. Proc Natl Acad Sci U S A 2009;106:19485–90.
10. Rouhi P, Jensen LD, Cao Z, Hosaka K, Lanne T, Wahlberg E, et al. Hypoxia-induced metastasis model in embryonic zebrafish. Nat Protoc 2010;5:1911–8.
11. Wang J, Cao Z, Zhang XM, Nakamura M, Sun M, Hartman J, et al. Novel mechanism of macrophage-mediated metastasis revealed in a zebrafish model of tumor development. Cancer Res 2015;75:306–15.
12. Lawson ND, Weinstein BM. In vivo imaging of embryonic vascular development using transgenic zebrafish. Dev Biol 2002;248:307–18.
13. Yang Y, Andersson P, Hosaka K, Zhang Y, Cao R, Iwamoto H, et al. The PDGF-BB-SOX7 axis-modulated IL-33 in pericytes and stromal cells promotes metastasis through tumour-associated macrophages. Nat Commun 2016;7:11385.
14. Lim S, Hosaka K, Nakamura M, Cao Y. Co-option of pre-existing vascular beds in adipose tissue controls tumor growth rates and angiogenesis. Oncotarget 2016;7:38282–91.
15. Hosaka K, Yang Y, Seki T, Fischer C, Dubey O, Fredlund E, et al. Pericyte-fibroblast transition promotes tumor growth and metastasis. Proc Natl Acad Sci U S A 2016;113:E5618–27.
16. Yang Y, Zhang Y, Iwamoto H, Hosaka K, Seki T, Andersson P, et al. Discontinuation of anti-VEGF cancer therapy promotes metastasis through a liver revascularization mechanism. Nat Commun 2016;7:12680.
17. Seki T, Hosaka K, Lim S, Fischer C, Honek J, Yang Y, et al. Endothelial PDGF-CC regulates angiogenesis-dependent thermogenesis in beige fat. Nat Commun 2016;7:12152.
18. Zhang Y, Yang Y, Hosaka K, Huang G, Zang J, Chen F, et al. Endocrine vasculatures are preferable targets of an antitumor ineffective low dose of anti-VEGF therapy. Proc Natl Acad Sci U S A 2016;113:4158–63.
19. Chen X, Wang J, Cao Z, Hosaka K, Jensen L, Yang H, et al. Invasiveness and metastasis of retinoblastoma in an orthotopic zebrafish tumor model. Sci Rep 2015;5:10351.
20. Yang X, Zhang Y, Hosaka K, Andersson P, Wang J, Tholander F, et al. VEGF-B promotes cancer metastasis through a VEGF-A-independent mechanism and serves as a marker of poor prognosis for cancer patients. Proc Natl Acad Sci U S A 2015;112:E2900–9.
21. Lim S, Zhang Y, Zhang D, Chen F, Hosaka K, Feng N, et al. VEGFR2-mediated vascular dilation as a mechanism of VEGF-induced anemia and bone marrow cell mobilization. Cell Rep 2014;9:569–80.
22. Hosaka K, Yang Y, Seki T, Nakamura M, Andersson P, Rouhi P, et al. Tumour PDGF-BB expression levels determine dual effects of anti-PDGF drugs on vascular remodelling and metastasis. Nat Commun 2013;4:2129.
23. Dong M, Yang X, Lim S, Cao Z, Honek J, Lu H, et al. Cold exposure promotes atherosclerotic plaque growth and instability via UCP1-dependent lipolysis. Cell Metab 2013;18:118–29.
24. Lim S, Honek J, Xue Y, Seki T, Cao Z, Andersson P, et al. Cold-induced activation of brown adipose tissue and adipose angiogenesis in mice. Nat Protoc 2012;7:606–15.
25. Xue Y, Lim S, Yang Y, Wang Z, Jensen LD, Hedlund EM, et al. PDGF-BB modulates hematopoiesis and tumor angiogenesis by inducing erythropoietin production in stromal cells. Nat Med 2011;18:100–10.
26. Cao Z, Jensen LD, Rouhi P, Hosaka K, Lanne T, Steffensen JF, et al. Hypoxia-induced retinopathy model in adult zebrafish. Nat Protoc 2010;5:1903–10.

27. Hedlund EM, Hosaka K, Zhong Z, Cao R, Cao Y. Malignant cell-derived PlGF promotes normalization and remodeling of the tumor vasculature. Proc Natl Acad Sci U S A 2009;106:17505–10.
28. Jensen LD, Cao Z, Nakamura M, Yang Y, Brautigam L, Andersson P, et al. Opposing effects of circadian clock genes bmal1 and period2 in regulation of VEGF-dependent angiogenesis in developing zebrafish. Cell Rep 2012;2:231–41.
29. O'Reilly MS, Holmgren L, Shing Y, Chen C, Rosenthal RA, Moses M, et al. Angiostatin: a novel angiogenesis inhibitor that mediates the suppression of metastases by a Lewis lung carcinoma. Cell 1994;79:315–28.
30. Cao Y, O'Reilly MS, Marshall B, Flynn E, Ji RW, Folkman J. Expression of angiostatin cDNA in a murine fibrosarcoma suppresses primary tumor growth and produces long-term dormancy of metastases. J Clin Invest 1998;101:1055–63.
31. Correa D, Somoza RA, Lin P, Schiemann WP, Caplan AI. Mesenchymal stem cells regulate melanoma cancer cells extravasation to bone and liver at their perivascular niche. Int J Cancer 2016;138:417–27.
32. Kuzet SE, Gaggioli C. Fibroblast activation in cancer: when seed fertilizes soil. Cell Tissue Res 2016;365:607–19.
33. Du H, Chen D, Zhou Y, Han Z, Che G. Fibroblast phenotypes in different lung diseases. J Cardiothorac Surg 2014;9:147.
34. Aboussekhra A. Role of cancer-associated fibroblasts in breast cancer development and prognosis. Int J Dev Biol 2011;55:841–9.
35. Jodele S, Blavier L, Yoon JM, DeClerck YA. Modifying the soil to affect the seed: role of stromal-derived matrix metalloproteinases in cancer progression. Cancer Metastasis Rev 2006;25:35–43.
36. Duda DG, Duyverman AM, Kohno M, Snuderl M, Steller EJ, Fukumura D, et al. Malignant cells facilitate lung metastasis by bringing their own soil. Proc Natl Acad Sci U S A 2010;107:21677–82.
37. Karnoub AE, Dash AB, Vo AP, Sullivan A, Brooks MW, Bell GW, et al. Mesenchymal stem cells within tumour stroma promote breast cancer metastasis. Nature 2007;449:557–63.
38. Cao Y. Opinion: emerging mechanisms of tumour lymphangiogenesis and lymphatic metastasis. Nat Rev Cancer 2005;5:735–43.